PHYSICAL REVIEW B VOLUME 61, NUMBER 24 15 JUNE 2000-II

Understanding reflectance anisotropy: Surface-state signatures and bulk-related features in the optical spectrum of InP(001)(2×4)

W. G. Schmidt*
Department of Physics, North Carolina State University, Raleigh, North Carolina 27695-8202

N. Esser, A. M. Frisch, and P. Vogt
Institut für Festkörperphysik, Technische Universität Berlin, Hardenbergstraße 36, 10623 Berlin, Germany

J. Bernholc
Department of Physics, North Carolina State University, Raleigh, North Carolina 27695-8202

F. Bechstedt
IFTO, Friedrich-Schiller-Universität Jena, Max-Wien-Platz 1, 07743 Jena, Germany

M. Zorn
Institut für Festkörperphysik, Technische Universität Berlin, Hardenbergstraße 36, 10623 Berlin, Germany

Th. Hannappel, S. Visbeck, and F. Willig
Hahn-Meitner-Institut, CD, Glienicker Straße 100, 14109 Berlin, Germany

W. Richter
Institut für Festkörperphysik, Technische Universität Berlin, Hardenbergstraße 36, 10623 Berlin, Germany

(Received 29 March 2000)

A detailed analysis based on *first-principles* calculations with self-energy corrections is combined with photoemission spectroscopy to determine the origin of features observed in reflectance anisotropy spectroscopy (RAS) at semiconductor surfaces. Using the InP(001)(2×4) surface as a model case we obtain quantitative agreement between slab calculations and low-temperature RAS measurements. We find the contributions to the anisotropy signal related either directly to surface states or to transitions between surface perturbed bulk wave functions. Our results demonstrate the high sensitivity of RAS to the surface structure and chemistry and show that the absorption processes causing the anisotropy signal take place in the uppermost few atomic layers of the substrate.

Reflectance anisotropy (difference) spectroscopy (RAS/RDS) is a versatile and powerful tool for monitoring surface processes in various environments.[1] Much work has been dedicated to clarifying the origin of the reflectance anisotropy. More than a decade ago it was shown that the anisotropy may be related to electronic surface states.[2] Aspnes and Studna[3] discriminated between two types of RAS components: ''intrinsic'' contributions from surface effects on bulk states and ''extrinsic'' contributions related to the surface structure. The latter are particularly interesting from surface science as well as from technological points of view, as they allow to correlate atomic surface structure and optical anisotropy.

The usual theoretical approach to study RAS on a microscopic scale employs slab calculations, where the surface is modeled by a few atomic layers. These calculations, however, often fail to reproduce the measured data satisfactorily. This is mainly due to (i) convergence problems caused by the numerical expense required for calculations of surface optical properties, and (ii) the difficulty to account for the many-particle effects in the spectra in an efficient yet accurate manner. Recent attempts to overcome these problems include a combination of *first-principles* total energy with tight-binding electronic structure calculations,[4] the application of a scissors operator,[5] and a linear parametrization of the quasiparticle shifts with respect to the surface localization of the corresponding electronic states.[6] The difficulty in theoretical modeling are partially responsible for an ongoing and controversial debate[7] about the physical mechanisms responsible for the reflectance anisotropy. Alternative explanations of the surface optical anisotropy were put forward. A dynamic photon-induced localization of the initial and final states over the range of the penetration depth of light of several hundred Angstroms was suggested to account for anisotropy signals close to the bulk critical point (CP) energies.[8] In Ref. 9 another long-range effect, the quenching of bulk-state wave functions near the surface, was made responsible for the appearance of peaks at bulk CP energies in the surface spectra. Obviously, the full exploitation of the technological potential of RAS requires to clarify the origin of the anisotropy signal and renders its accurate theoretical modeling a much needed and challenging task.

We combine *ab initio* calculations that include self-energy corrections with angle resolved photoemission spectroscopy (ARPES) and low-temperature RAS to achieve a thorough understanding of the anisotropy spectrum of the

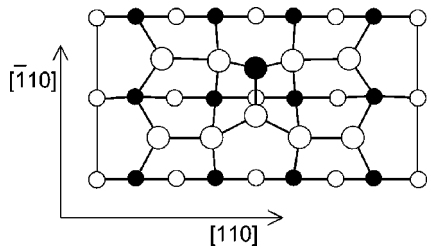

FIG. 1. Top view of the In-rich InP(001)(2×4) surface reconstruction. Empty (filled) circles represent In (P) atoms. Large (small) symbols indicate positions in the first and second (third and fourth) atomic layers.

In-rich InP(001)(2×4) surface. We will show that both intrinsic and extrinsic contributions appear in the RAS and are accessible to well-converged slab calculations. Surface state signatures in the spectrum, not addressed by the absorption mechanisms proposed in Refs. 8 and 9, are identified and traced to specific surface bonds.

The atomic[10,11] and electronic structure[12,13] of the In-rich InP(001) surface is well understood. Mixed In-P dimers oriented along [$\bar{1}\bar{1}$0] terminate the surface (Fig. 1). In-In bonds along [110] form in the second layer. The RAS and ARPES experiments discussed in the following were performed on homoepitaxial InP(001) layers grown by metal-organic vapor phase epitaxy (MOVPE). The uncontaminated samples were transferred after growth to different ultra high vacuum (UHV) analysis chambers for surface characterization.[14] The (2×4) reconstructed, In-terminated surfaces were either prepared by annealing the samples in UHV or directly by MOVPE growth.[15]

Results for the optical anisotropy measured at 300 and 25 K are shown in the lower part of Fig. 2. The room temperature data agree with earlier findings:[16] There is a strong negative anisotropy around 1.8 eV and further features appear close to the E_1 and E_0' CP energies and between them (denoted A). As expected, the features in the low-temperature spectrum are blue-shifted with respect to the 300 K measurement, and sharpened. The negative anisotropy at low energies splits into peaks at 1.9, 2.1, and 2.6 eV (denoted $S1$, $S2$ and $S3$).

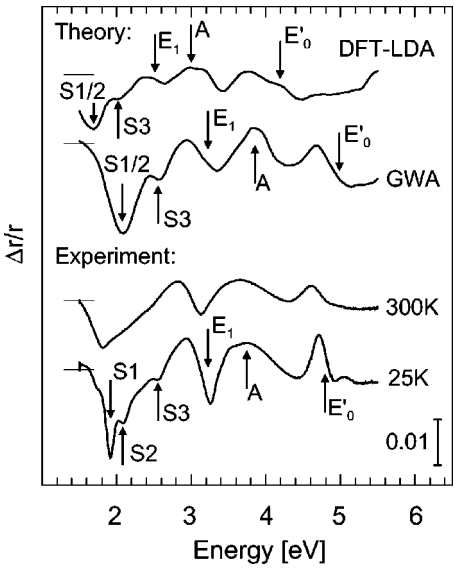

FIG. 2. RAS spectra [Re{$(r_{[\bar{1}10]}-r_{[110]})/\langle r\rangle$}] for the In-rich InP(001)(2×4) surface. Calculated spectra are shown as obtained within DFT-LDA and GWA. Measurements were performed at 300 and 25 K. Bulk CP energies and surface-related features are indicated.

In a previous theoretical study on InP(001) (Ref. 17) the measured RAS was roughly reproduced. However, the fine structure was not resolved and the energetic positions, in particular of the high-energy features, were not in accordance with experiment. We address these issues in the present calculation by using a much denser **k**-point mesh and including self-energy effects that were formerly ignored. In detail, we start from first-principles pseudopotential calculations using density-functional theory in the local-density approximation (DFT-LDA). To deal efficiently with the large surface unit cell and the many states required for the calculation of the dielectric function we use a massively parallel real-space finite-difference method.[18] A multigrid technique is used for convergence acceleration. The surface is modeled by a periodic supercell containing 12 atomic layers, the bottom layer saturated with pseudohydrogens, and a vacuum region equivalent to eight layers. The 10 upper layers of the slab were relaxed until all calculated forces were below 25 meV/Å. The **k**-point sampling corresponds to 1024 points in the (1×1) surface Brillouin zone (SBZ). Further details of the DFT-LDA calculations are the same as in Refs. 17 and 19.

The inclusion of self-energy effects, neglected in DFT-LDA, requires the replacement of the LDA exchange and correlation potential by the nonlocal and energy-dependent self-energy operator $\Sigma(\mathbf{r},\mathbf{r}';E)$ (see, e.g., Ref. 20). Even in the lowest, so-called GW approximation (GWA), where Σ is expressed as convolution of the single-particle propagator G and the dynamically screened Coulomb interaction W, its calculation is a formidable task, in particular for the large number of states entering the surface dielectric function. Therefore, we introduce further approximations and use a model dielectric function[21] to calculate W. The local-field effects are approximated by the dependence of the dielectric function on the local charge density and a single plasmon pole approximation accounts for the energy dependence (see Ref. 21 for details). This approach allows the calculation of the quasiparticle shifts for all electronic states and at all considered **k** points. In the case of bulk InP it opens the E_0 gap at Γ from 0.9 eV in DFT-LDA to 1.4 eV. The transition energies E_1 and E_0' are shifted from 2.5 to 3.2 eV and from 4.2 to 5.0 eV, respectively. These values are in good agreement with the E_0, E_1 and E_0' energies of 1.4, 3.3 and 4.8 eV measured at 30 K.[22] Our GW model requires the input of the dielectric constant ϵ_∞. The inaccuracies caused by the use of the bulk dielectric constant for surface GW calculations, however, are very small.[23] Following Del Sole,[24] the electronic structure obtained in DFT-LDA/GWA is then finally used to calculate the optical anisotropy.

The resulting spectra are shown in the upper part of Fig. 2. For low photon energies we obtain two pronounced negative peaks (denoted $S1/2$ and $S3$). In the high-energy region features appear close to the E_1 and E_0' energies. In between

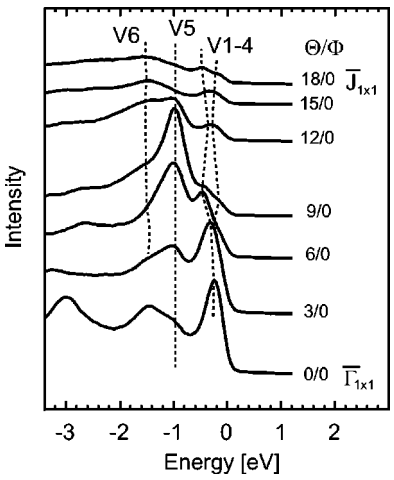

FIG. 3. Valence band spectra of InP(001)(2×4) taken at a photon energy of 21.4 eV along $\bar{\Gamma}$-$\bar{J}$. Labeled surface states refer to Table I. The binding energy is given with respect to the VBM.

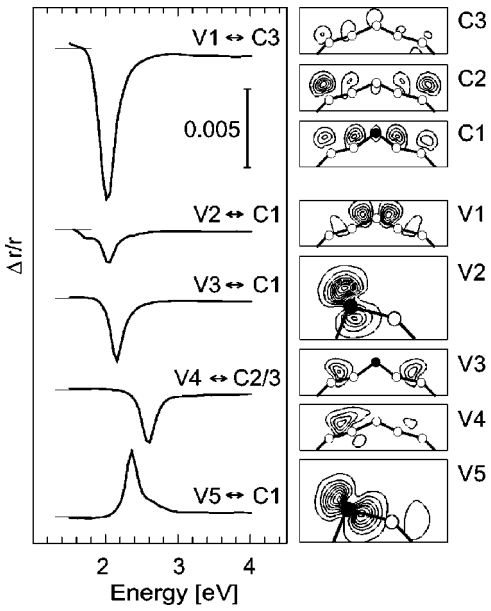

FIG. 4. Left: Calculated RAS due to transitions between specific surface states as indicated. Right: Orbital character of the corresponding states at $\bar{K}$ (spacing 10^{-3} Bohr^{-3}).

a structure A occurs. Together they form a characteristic ''three-buckle'' shape. Separating spatially the contributions to the optical anisotropy from different slab regions,[17,19] we find that $S1/2$ and $S3$ originate entirely from the uppermost 4 atomic layers. This is consistent with experiment, as the measured negative anisotropy for low energies is extremely stoichiometry dependent and therefore surface related.[16] The features at the CP energies arise from transitions between bulk-like electronic states that are perturbed by the surface. This holds also for A, which is mainly caused by transitions involving the bulk bonds down to nine layers below the surface. In earlier calculations[17,19] we have shown that these high-energy features are rather insensitive to the atomic surface structure, which agrees with experiment,[16] where changes in the surface conditions had very little effect on the three-buckle shape.

The major experimental features are qualitatively reproduced in the DFT-LDA calculations, although at much lower photon energies. The improved **k**-point sampling resolves the $S1/2$ and $S3$ features. Inclusion of self-energy effects shifts the peak positions non-uniformly to higher energies, aligning them with experiment within a few tenths of an eV. The shifts for the bulk related features are between 0.7 and 1.0 eV, somewhat larger than the shifts of 0.4–0.5 eV for the surface peaks. The changes of the line shape due to self-energy effects distinctly improve the agreement with experiment.

In order to trace the origin of the surface-related anisotropies in detail, we analyze our ARPES data (Fig. 3) using the calculated electronic structure. We find several weakly dispersing surface bands close to the bulk valence band maximum (VBM). A strong surface resonance shows up at -0.9 eV and another one is found at -1.5 eV. These observations agree with our calculations. Calculated energies of near-gap surface states (see the right panel of Fig. 4) are given in Table I. We find four partially bound surface states, $V1-4$, close to the VBM. $V1$ is formed by the bonds between first and second-layer cations, $V2$ corresponds to the P dangling bond at the mixed dimer and $V3$ arises from the second-layer In-In bonds at the anion site of the mixed dimer. $V4$ is complementary to $V3$ and comparatively weakly localized at the second-layer cations at the cation site of the mixed dimer. The latter two states are degenerate with bulk bands for most parts of the SBZ (see also Ref. 12). In addition, there are surface resonances. The strongly localized mixed-dimer bond, $V5$, forms a very flat band at about -0.8 to -0.9 eV. The bonds between the uppermost P and the second-layer In atoms, $V6$, disperse in energy between -1.3 and -1.6 eV. The lowest unoccupied surface states, $C1-3$, correspond to empty dangling bonds localized at the surface cations. $C1$ is also localized at the mixed dimer (see also Fig. 5 in Ref. 17). Its energy agrees with the available inverse photoemission data.[13]

In order to gain an intuitive understanding of the optical anisotropy, we investigated the existence of surface state ''signatures'' by calculating the RAS due to transitions within pairs of the above identified surface states. We find that some of these transitions give rise to pronounced anisotropy features, the superposition of which nearly accounts for the entire surface contribution to the spectrum. Figure 4 shows the calculated contribution to the RAS from transitions involving $V1-5$ and $C1-3$. The strongest anisotropy contribution (at 2.0 eV) comes from the bonds between first- and second-layer cations, $V1$. The strongly surface-localized P dangling bond, $V2$, on the other hand, contributes only weakly. There are also anisotropies due to transitions between the second-layer In-In bonds, $V3$ and $V4$, and the empty In dangling bonds $C1$ and $C2/3$. We calculate the corresponding peak positions at 2.2 and 2.6 eV, respectively. Finally, a positive anisotropy feature at 2.4 eV is caused by transitions related to the mixed-dimer bond $V5$. The above analysis provides a complete understanding of the surface features of the optical anisotropy: $S1$ is caused by the bonds between first- and second-layer cations. $S2$ arises from transitions mainly involving the second-layer In-In bonds. The symmetry break induced by the mixed dimer on the In-In bonds of the second atomic layer together with the dimer

TABLE I. Surface state energies (in eV) at high-symmetry and special **k** points with respect to the VBM calculated in GWA. Only clearly surface localized states ($|\psi|^2_{max} \geq 2\times10^{-3}$ Bohr^{-3}) are considered.

	$V6$	$V5$	$V4$	$V3$	$V2$	$V1$	$C1$	$C2$	$C3$
$\bar{\Gamma}$	−1.6	−0.9			−0.3	−0.2	1.5	2.2	
$\bar{K}$	−1.4	−0.9	−0.4	−0.2	−0.1	0.2	2.1	2.3	2.5
$(0.5\bar{J},0.25\bar{J'})$		−0.7	−0.7		−0.1	0.0	1.6	1.9	2.0
$(0.5\bar{J},0.75\bar{J'})$		−0.8		−0.2	−0.1	0.1	1.9	2.1	2.2

bond itself are responsible for $S3$. Although an interpretation of RAS based entirely on the orientation of surface bonds may be misleading,[4,5] in the present case the numerical analysis is consistent with such a picture: Assuming a larger polarizability along the bond direction, negative anisotropies are expected for the In-In bonds, oriented along $[110]$, and positive features for the dimer bond, oriented along $[\bar{1}10]$.

The calculated RAS in GWA reproduces the overall experimental data very well, but still deviates in some details. These discrepancies are related to numerical limitations: In the present calculation the distinct contributions from $V1$ and $V3$ at 2.0 and 2.2 eV are not resolved. Instead, we obtain one relatively broad minimum at 2.1 eV, due to the finite energy broadening necessary to account for the still limited number of wave vectors used to sample the SBZ. Furthermore, the LDA-like treatment of local-field effects in our GW model only approximates the surface screening. Electron-hole interaction and spin-orbit coupling are left out completely. The latter is likely to affect the line shape in particular at the bulk CPs. Finally, the calculations are performed for an ideal surface, neglecting the observed defects and domain boundaries.[10]

In conclusion, using InP$(001)(2\times4)$ as a model case, we have shown that all features seen in RAS spectra can be identified and quantitatively well described by slab calculations which take the electronic transitions within the uppermost atomic layers of the substrate into account. Both the measured extrinsic as well as the intrinsic spectral features are reproduced without any need to invoke longe-range effects such as photon-induced localization or quenching of bulk states. Extrinsic anisotropy features were explained in terms of transitions involving specific surface bonds, and ''intrinsic'' anisotropies at higher photon energies were assigned to subsurface transitions between surface perturbed bulk-like states. Inclusion of self-energy effects and using a very dense **k**-point mesh lead to a very good agreement between calculation and experiment.

We acknowledge support by DFG (Schm 1361/1-1, Es 127/4-1), ONR (N00014-96-I-0161), and NSF (DMR 9408437) as well as grants of computer time from the DoD Challenge Program and the North Carolina Supercomputing Center.

*Permanent address: IFTO, FSU Jena, Max-Wien-Platz 1, 07743 Jena, Germany. Email: W.G.Schmidt@ifto.physik.uni-jena.de

[1] W. Richter and J. T. Zettler, Appl. Surf. Sci. **101**, 465 (1996).
[2] P. Chiaradia, A. Cricenti, S. Selci, and G. Chiarotti, Phys. Rev. Lett. **52**, 1145 (1984).
[3] D. E. Aspnes and A. A. Studna, Phys. Rev. Lett. **54**, 1956 (1985).
[4] A. I. Shkrebtii *et al.*, Phys. Rev. Lett. **81**, 721 (1998).
[5] L. Kipp *et al.*, Phys. Rev. Lett. **76**, 2810 (1996).
[6] O. Pulci, G. Onida, R. Del Sole, and L. Reining, Phys. Rev. Lett. **81**, 5374 (1998).
[7] R. Del Sole and G. Onida, Phys. Rev. B **60**, 5523 (1999), and references therein.
[8] L. Mantese, K. A. Bell, D. E. Aspnes, and U. Rossow, Phys. Lett. A **253**, 93 (1999).
[9] K. Uwai and N. Kobayashi, Phys. Rev. Lett. **78**, 959 (1997).
[10] C. D. MacPherson, R. A. Wolkow, C. E. J. Mitchell, and A. B. McLean, Phys. Rev. Lett. **77**, 691 (1996).
[11] W. G. Schmidt *et al.*, Phys. Rev. B **57**, 14 596 (1998).
[12] W. G. Schmidt and F. Bechstedt, Surf. Sci. **409**, 474 (1998).
[13] S. Riese, E. Milas, and H. Merz, Surf. Sci. **270**, 833 (1992).
[14] T. Hannappel *et al.*, Appl. Phys. A: Mater. Sci. Process. **69**, 427 (1999).
[15] T. Hannappel *et al.* (unpublished).
[16] D. Pahlke *et al.*, Phys. Rev. B **56**, R1661 (1997); M. Zorn *et al.*, Appl. Phys. A: Mater. Sci. Process. **65**, 333 (1997); K. B. Ozanyan *et al.*, J. Appl. Phys. **82**, 474 (1997).
[17] W. G. Schmidt, E. L. Briggs, J. Bernholc, and F. Bechstedt, Phys. Rev. B **59**, 2234 (1999).
[18] E. L. Briggs, D. J. Sullivan, and J. Bernholc, Phys. Rev. B **54**, 14 362 (1996).
[19] A. M. Frisch *et al.*, Phys. Rev. B **60**, 2488 (1999).
[20] M. S. Hybertsen and S. G. Louie, Phys. Rev. B **34**, 5390 (1986).
[21] F. Bechstedt, R. Del Sole, G. Cappellini, and L. Reining, Solid State Commun. **84**, 765 (1992).
[22] P. Lautenschlager, M. Garriga, and M. Cardona, Phys. Rev. B **36**, 4813 (1987).
[23] J. E. Northrup, Phys. Rev. B **47**, 10 032 (1993).
[24] R. Del Sole, Solid State Commun. **37**, 537 (1981).